17th Brazilian Congress of Thermal Sciences and Engineering
November 25th-28th, 2018, Águas de Lindóia, SP, Brazil

ENCIT-2018-0123
EVALUATION OF THE WSGG MODEL ACCURACY AS A FUNCTION OF PATH LENGTH IN NON-ISOTHERMAL, NON-HOMOGENEOUS MEDIA

Felipe Ramos Coelho
Guilherme Crivelli Fraga
Francis Henrique Ramos França
Universidade Federal do Rio Grande do Sul, Department of Mechanical Engineering, Av. Paulo Gama, 110, Porto Alegre, RS, Brazil
felipe.coelho@ufrgs.br
guilhermecfraga@ufrgs.br
frfranca@mecanica.ufrgs.br

Abstract. *This study evaluates the weighted-sum-of-gray-gases (WSGG) model accuracy for mixtures of CO_2 and H_2O, with path lengths ranging from 0.25 to 30 m, in non-isothermal, non-homogeneous conditions. The WSGG coefficients from several authors are used considering a mixture with fixed mole ratio of 2/1, representing typical products of stoichiometric combustion of methane in air. Previous results show that all the coefficients are capable of accurately predicting emittance data when compared to the line-by-line (LBL) benchmark solution for the whole path length range. However, radiative heat flux and volumetric source validation was only performed for a limited number of path lengths. The main objective of this study is to extend these calculations for a path length range of 0.25 to 30 m and understand how both quantities are affected by it. Results show how the WSGG normalized average deviations from the LBL benchmark vary as a function of path length. These normalized deviations are then used to determine path length ranges of applicability (PLRAs) for all the WSGG coefficients, aiming to obtain a maximum of 5% normalized average deviation for both radiative heat flux and volumetric source. A second approach is also employed to obtain PLRAs considering a maximum average deviation of 10%. Results show that the radiative heat flux is the limiting factor for determining the WSGG coefficients PLRAs, since deviations are overall higher than those of the radiative volumetric source. Furthermore, this study shows that most WSGG coefficients were applicable to the whole path length range when solving isothermal and homogeneous conditions, but only a few had wide PLRAs on non-isothermal and non-homogeneous conditions, even when considering maximum average deviations of 10%. As a consequence, the PLRAs for radiative heat flux and volumetric source calculations are overall smaller than those recommended by other authors based on total emittance results, emphasizing the importance of studying the path length effect on the WSGG accuracy and applicability.*

Keywords: *WSGG, LBL, path length, ranges of applicability, HITEMP2010.*

1. INTRODUCTION

Thermal radiation is often a very important form of heat exchange in combustion processes, due to the high temperatures resulted from the reaction and the generation of products that act as participating gases in such conditions. The radiative heat transfer energy balance on a participating gas results in the radiative transfer equation (RTE), which dictates how the spectral radiation intensity varies along the domain. The solution of the RTE is complex since it requires spatial, directional, and spectral integration. Spectral integration is particularly challenging, mainly due to the highly irregular behavior of the absorption coefficient along the spectrum, which is also dependent on the thermodynamic state of the gas. Currently, the most accurate form of spectral integration of the RTE is the line-by-line (LBL) method, which considers all the variations of the spectral properties along the spectrum and is often regarded as a benchmark solution. The spectral properties of the participant gases are usually taken from high-resolution spectral databases such as HITEMP2010 (Rothman *et al*., 2010).

However, because of the highly irregular spectral dependence of the absorption coefficient, the LBL method's computational cost ends up being too high for most applications, especially when the thermodynamic state of the gas varies along the domain. Because of this limitation, radiation in participant gases is more commonly solved using spectral gas models, simplifying the spectral integration. The weighted-sum-of-gray-gases (WSGG) model, proposed by Hottel and Sarofim (1967), is an example of spectral gas model which simplifies the original behavior of the absorption coefficient of a participating gas considering a few gray gases with uniform pressure absorption coefficient. Smith *et al.*, 1982, proposed a methodology for obtaining WSGG coefficients based on a polynomial fit of the weighting factors as a function of temperature, and generated new WSGG coefficients for fixed ratio mixtures of CO_2 and H_2O considering three gray gases. Using a similar methodology, Dorigon *et al*., 2013, generated new coefficients based on

the HITEMP2010 database considering four gray gases for fixed ratio mixtures of CO_2 and H_2O, at atmospheric pressure and for a wide range of temperatures and pressure path lengths. The fixed mole ratios used to generate the coefficients from Smith *et al*., 1982, and Dorigon *et al*., 2013, were based on stoichiometric combustion of methane and oil, both in atmospheric air. Krishnamoorthy, 2010, also generated new fixed ratio WSGG coefficients, but then extending the mole ratio ranges in order to better represent the H_2O/CO_2 ratios present in Sandia Flame D, which is a methane and air turbulent jet flame experimentally investigated by Barlow and Frank, 1998. An alternative to the classic fixed ratio mixture approach was proposed by Johansson *et al*., 2011, generating new WSGG coefficients which are function of the H_2O/CO_2 mole ratio and are valid for ratios ranging from 0.125 to 2. Refined WSGG coefficients were also generated by Yin, 2013, expanding the temperature and the mole ratio ranges proposed by Smith *et al*., 1982. Recently, there has been a considerable interest in applying the WSGG model to high total pressure conditions. Bahador and Sunden, 2008, developed a new WSGG model applicable to high total pressure conditions considering three gray gases based on spectroscopic databases. Coelho and França, 2018, generated new WSGG correlations considering four gray gases, based on HITEMP2010, and applicable to high total pressure conditions for fixed ratio mixtures, using a similar methodology as the one employed by Dorigon *et al*., 2013. There has also been a significant interest in developing new WSGG coefficients applicable to oxy-fuel conditions by several authors (Yin *et al*., 2010; Kangwanpongpan *et al*., 2012; Krishnamoorthy, 2012; Bordbar *et al*., 2014; Guo *et al*., 2015). In summary, WSGG is an extensively studied spectral gas model with various correlations available on the literature, which are mostly valid for wide ranges of applications, leading to sufficiently accurate results despite the simplicity of the model. The applicability of the WSGG coefficients is usually given by the mole ratio and the path length ranges. However, this path length range is often determined solely based on total emittance results while the RTE is only solved for some limited values of path length.

This study evaluates the RTE solution for radiative heat flux and volumetric source comparing the WSGG coefficients from several authors (Smith *et al*., 1982; Dorigon *et al*., 2013; Coelho and França, 2018; Johansson *et al*., 2011; Krishnamoorthy, 2010; Bahador and Sunden, 2008; Yin, 2013) with the LBL benchmark solution, for path lengths from 0.25 to 30 m, in non-isothermal, non-homogeneous mixtures of CO_2 and H_2O. The main objective is to verify if the good accuracy of the emittance results reported by the authors for this path length range is also obtainable for radiative heat flux and volumetric source results when analyzing four different test cases. The influence of the path length on deviations is analyzed for all test cases, and based on these results, path length ranges of applicability (PLRAs) are suggested for each case and for each set of WSGG coefficients.

2. METHODOLOGY

The RTE results from an energy balance of the radiative heat transfer in a participating media, which for a one dimensional and non-scattering media is given by (Siegel and Howell, 2002)

$$\frac{dI_\eta(x)}{dx} = -\kappa_\eta(x) I_\eta(x) + \kappa_\eta(x) I_{\eta b}(x) \tag{1}$$

in which κ_η is the absorption coefficient, in m^{-1}, and I_η and $I_{\eta b}$ represent the spectral intensity and the blackbody radiation intensity, respectively, in $W/(m^2\ cm^{-1})$. The RTE represents how the spectral radiation intensity varies along the participant media with the attenuation effect given by the negative term and the augmentation given by the positive term in Eq. (1). The absorption coefficient κ_η is calculated from

$$\kappa_\eta = NYC_\eta \tag{2}$$

where N is the gas molar density, in molecule/cm³, Y is the mole fraction, and $C\eta$ is the absorption cross-section of the gas, in cm²/molecule. In this study, the absorption cross-sections for the LBL solution are obtained from HITEMP2010 database for mole fractions of $Y_c = 0.1$ for CO_2 and $Y_w = 0.2$ for H_2O, temperatures ranging from 400 K to 2500 K, and atmospheric total pressure. These mole fractions represent typical stoichiometric methane combustion with air (Dorigon *et al*., 2013, Cassol *et al*., 2014, Coelho and França, 2018) resulting in a mole ratio of 2. The spectrum wavenumber ranges from 0 cm^{-1} to 10000 cm^{-1} and is divided in 150000 elements. Spectral lines are modeled by the Lorentz profile, considering that collision between the molecules is the main reason for spectral line broadening.

The WSGG model replaces the continuous behavior of the absorption coefficient by a finite number of gray gases J with constant pressure absorption coefficient $\kappa_{p,j}$ plus transparent windows. Each gray gas j covers a portion of the spectrum $\Delta\eta_j$ which is not necessarily continuous (Dorigon *et al*., 2013). The model also assumes that the temperature dependency is present on the temperature dependent weighting coefficients $a_j(T)$ instead of the absorption coefficient. Under these assumptions, the RTE in Eq. (1) applied over a portion of the spectrum $\Delta\eta_j$ related to the j-th gray gas results in

$$\frac{dI_j(x)}{dx} = -\kappa_{p,j} p_a(x) I_j(x) + \kappa_{p,j} p_a(x) a_j(T) I_b(T) \tag{3}$$

where p_a is the partial pressure of species a, in atm, a_j is the temperature dependent coefficient, dimensionless, and $I_b(T)$ is the total blackbody intensity, in W/m². The temperature dependent coefficient a_j is obtained from

$$a_j(T) = \sum_{k=0}^{K} b_{j,k} T^k \tag{4}$$

where $b_{j,k}$ are the polynomial coefficients of the WSGG model. In this study, the coefficients $b_{j,k}$ and $\kappa_{p,j}$ are taken from the set of coefficients developed by each author analyzed (Smith *et al*., 1982; Dorigon *et al*., 2013; Coelho and França, 2018; Johansson *et al*., 2011; Krishnamoorthy, 2010; Bahador and Sunden, 2008; Yin, 2013) for atmospheric pressure and mole ratio of 2.

The radiative heat flux and volumetric source are calculated for four test cases consisting of one dimensional problems of two infinite parallel walls with mixtures of CO_2 and H_2O between them. The plates have a distance L between them, which in this study varies from 0.25 to 30 m for all test cases. The CO_2/H_2O mixture distribution along the domain is dependent on the analyzed test case. Case 1 is a homogeneous mixture with $Y_c = 0.1$ and $Y_w = 0.2$, while Cases 2-4 are non-homogeneous mixtures with CO_2 mole fraction varying according to Eqs. (5)-(7), respectively.

$$Y_c(x) = 0.2 \sin^2(\pi x) \tag{5}$$

$$Y_c(x) = 0.2 \sin^2(2\pi x) \tag{6}$$

$$Y_c(x) = \begin{cases} 0.25 \sin^2(2\pi x) & \text{if } x \le 0.25 \\ 0.25\left(1 - \sin\left(\frac{2}{3}\pi\left(x - 0.25\right)\right)\right) & \text{if } x > 0.25 \end{cases} \tag{7}$$

In Cases 2-4, Y_w/Y_c is kept constant and equal to 2, the same ratio used to generate the WSGG coefficients. Since Y_w varies from 0 to 0.4 for Cases 2-3 and from 0 to 0.5 for Case 4, absorption spectra were generated for H_2O with Y_w = 0.01, 0.1, 0.2, 0.3, 0.4, and 0.6, using linear interpolation for intermediate mole fraction values. For CO_2, a simple linear relation based on the absorption cross-sections for $Y_c = 0.1$ was applied for other mole fractions ranging from 0 to 0.25, since CO_2 does not present considerable self-broadening effect (Cassol *et al*., 2014). The gas temperature distribution is also dependent on the analyzed test case. Case 1 has a uniform temperature distribution, with the gas mixture at 1100 K and the walls at 400 K. Cases 2-4 present non-uniform temperature distributions along the domain, which are given by Eqs. (8)-(10), respectively.

$$T(x) = 400K + (1400K) \sin^2(\pi x) \tag{8}$$

$$T(x) = 400K + (1400K) \sin^2(2\pi x) \tag{9}$$

$$T(x) = \begin{cases} 880\ \text{K} + 920\ \text{K} \sin^2(2\pi x) & \text{if } x \le 0.25 \\ 880\ \text{K} + 920\ \text{K}\left(1 - \sin^{3/2}\left(\frac{2}{3}\pi\left(x - 0.25\right)\right)\right) & \text{if } x > 0.25 \end{cases} \tag{10}$$

The radiative heat flux q_R'', in W/m², and volumetric source S_R, in W/m³, for the LBL method are obtained by integrating the RTE in Eq. (1) with the discrete ordinates method for a total of thirty directions. Balancing the forward and negative direction spectral intensities for the studied one dimensional problem, results in

$$q_R''(x) = \sum_{m=1}^{n_d} \int 2\pi \mu_m \omega_m \left[I_{\eta,m}^{+}(x) - I_{\eta,m}^{-}(x) \right] d\eta \tag{11}$$

$$S_R(x) = \sum_{m=1}^{n_d} \int_{\eta} \left\{ 2\pi\kappa_\eta \omega_m \left[I^+_{\eta,m}(x) + I^-_{\eta,m}(x) \right] - 4\pi\kappa_\eta I_{\eta b} \right\} d\eta \tag{12}$$

where μ_m is the direction cosine in direction m, ω_m is the quadrature weight for direction m, and $I^+_{\eta,m}$ and $I^-_{\eta,m}$ are the radiative spectral intensities in the forward direction $\mu_m > 0$ and backward direction $\mu_m < 0$, respectively. Since the walls are considered to be perfectly black, the boundary conditions in $x = 0$ and $x = L$ are $I^+_{\eta,m}(0) = I_{\eta b}(0)$ and $I^-_{\eta,m}(L) = I_{\eta b}(L)$. A similar integration using the same total directions is performed for the WSGG model RTE as presented in Eq. (3), leading to

$$q''_R(x) = \sum_{m=1}^{n_d} \sum_{j=1}^{n_g} 2\pi\mu_m \omega_m \left[I^+_{j,m}(x) - I^-_{j,m}(x) \right] \tag{13}$$

$$S_R(x) = \sum_{m=1}^{n_d} \sum_{j=1}^{n_g} \left\{ 2\pi\omega_m \kappa_j \left[I^+_{j,m}(x) + I^-_{j,m}(x) \right] - 4\pi\kappa_j a_j I_{\eta b} \right\} \tag{14}$$

in which $I^+_{j,m}$ and $I^-_{j,m}$ are the radiation intensities for gray gas j in forward direction $\mu_m > 0$ and backward direction $\mu_m < 0$, respectively. The boundary conditions for $x = 0$ and $x = L$ are $I^+_{j,m}(0) = a_j(0) I_{\eta b}(0)$ and $I^-_{j,m}(L) = a_j(L) I_{\eta b}(L)$.

The radiative heat flux q''_R and volumetric source S_R are calculated for the WSGG model using Eqs. (13) and (14) along with the WSGG coefficients, for distances L ranging from 0.25 to 30 m. These results are then compared to the LBL benchmark solutions using the previously obtained absorption cross-sections along with Eqs. (11) and (12), for the same distance range, and the normalized deviations between both methods is calculated as

$$\delta = \frac{\left| q''_{R,WSGG} - q''_{R,LBL} \right|}{máx \left| q''_{R,LBL} \right|} \tag{15}$$

$$\gamma = \frac{\left| S_{R,WSGG} - S_{R,LBL} \right|}{máx \left| S_{R,LBL} \right|} \tag{16}$$

These normalized deviations are then used to determine PLRAs, aiming to obtain ranges of L which contain a maximum of 5% average normalized deviation for both radiative heat flux and volumetric source. A second approach is also performed to determine PLRAs for maximum average deviations of 10%.

3. RESULTS

3.1 Case 1

The radiative heat flux and volumetric source results for the LBL benchmark and the WSGG solutions with L = 30 m are shown in Fig. 1 for Case 1. According to the figure, despite the distance between plates being L = 30 m, the WSGG results for radiative volumetric source are in great agreement with the LBL solution for all coefficients analyzed. However, there are higher deviations on the radiative heat flux results of some coefficients, especially the ones from Smith *et al*., 1982, and Yin, 2013. These higher deviations are consequence of the high distance between plates, as can be seen in Fig. 2, which shows the behavior of the WSGG average deviations for Case 1 as a function of L, ranging from 0.25 to 30 m. Figure 2a shows that the average deviations for radiative heat flux of some coefficients increase past a certain value of L (Smith *et al*., 1982; Yin, 2013; Krishnamoorthy, 2010; Johansson *et al*., 2011) while others decrease (Dorigon *et al*., 2013; Coelho and França, 2018; Bahador and Sunden, 2008). In fact, there seem to be no clear pattern of the radiative heat flux deviations behavior as a function of L for any of the models analyzed, most varying between increases and decreases and presenting local minima. This irregular behavior of the radiative heat flux deviations makes choosing the best model dependent on the desired L, as the WSGG model from Johansson *et al*., 2011,

presents the lowest deviations near L = 1 m, while the model from Coelho and França, 2018, presents lower deviations for higher values of L. The presence of local minima is interesting because, if their location could be predetermined, one could develop WSGG coefficients that present local minima near the desired values of L of specific applications. On the other hand, Fig. 2b shows that the radiative volumetric source deviations have a pattern of decreasing with L, with some models presenting local minima (Smith *et al.*, 1982; Yin, 2013). This effect is interesting since spectral models in general are expected to present a decrease in accuracy as the optical thickness increases. Despite the variety in patterns, Case 1 presents overall low deviations, with them being lower than 5% for most radiative heat flux results (except for some ranges of Smith *et al.*, 1982 and Yin, 2013 models) and lower than 2% for all radiative volumetric source results.

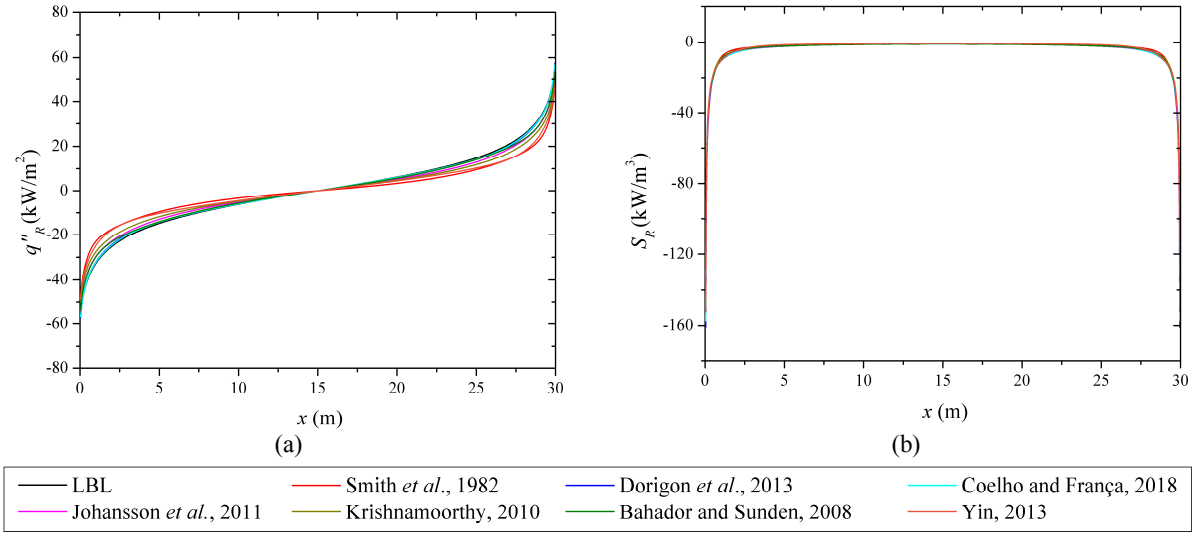

Figure 1. LBL and WSGG solutions for Case 1 with L = 30 m: (a) radiative heat flux; (b) radiative volumetric source.

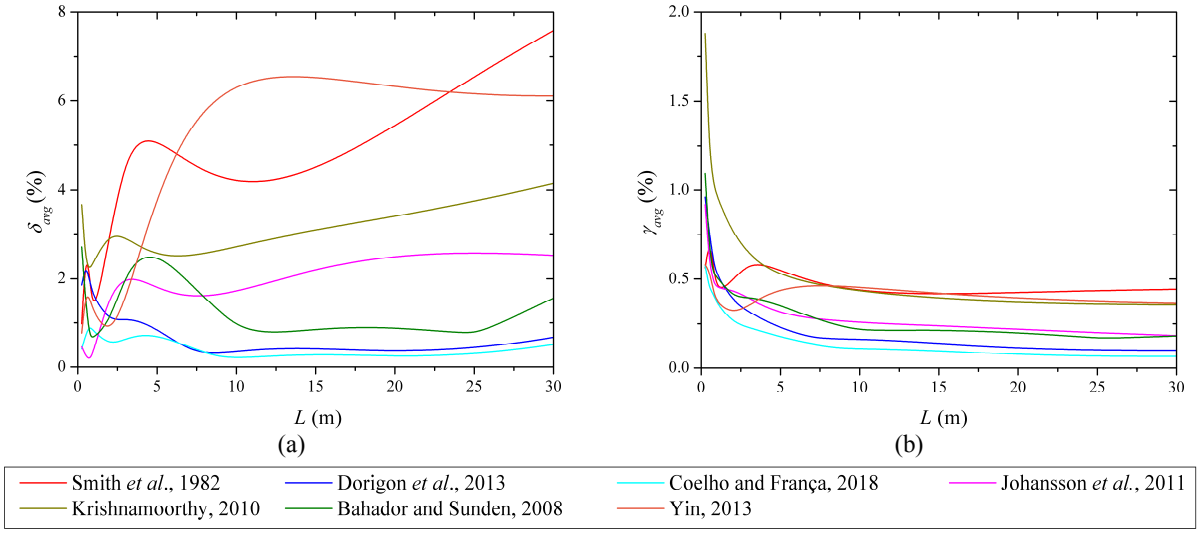

Figure 2. WSGG average deviations as function of L for Case 1 and for: (a) radiative heat flux; (b) radiative volumetric source.

3.2 Case 2

The radiative heat flux and volumetric source results for the LBL benchmark and the WSGG solutions with L = 30 m is shown in Fig. 3 for Case 2. According to the figure, these WSGG results are a lot worse than the ones observed on Case 1, which was expected since Case 2 involves non-uniform temperature and mole fraction profiles. Even the best performing models such as the ones from Dorigon *et al.*, 2013, and Coelho and França, 2018, show deviations considerably higher than those reported for lower values of L. Figure 3a shows that the WSGG model performs worse near the walls for the radiative heat flux while the radiative volumetric source has worse results near $x = L/2$ = 15 m. As

in Case 1, Smith *et al.*, 1982 and Yin, 2013 models show the worst performance among the others for L = 30 m, and this is also true for other values of L, as can be seen in Fig. 4, which shows the average deviations of Case 2 as a function of the distance between plates L. Figure 4a shows that radiative heat flux deviations increase with L, becoming higher than 10% for all models with L = 30 m and even higher than 30% for Smith *et al.*, 1982 and Yin, 2013 models. All models also present local minima for L < 5 m, with Johansson *et al.*, 2011 being the best performing model near L = 1 m and Dorigon, 2013 and Coelho and França, 2018 models performing best for higher values of L, in a similar way as observed in Case 1. Figure 4b shows that the pattern of the radiative volumetric source deviations is very similar, including the presence of local minima and the models which present the best results, but with overall lower magnitude, with average deviations between 4% and 10% for L = 30 m. It is interesting that the behavior of the radiative volumetric source deviations of Case 2 is the opposite as the one observed in Case 1.

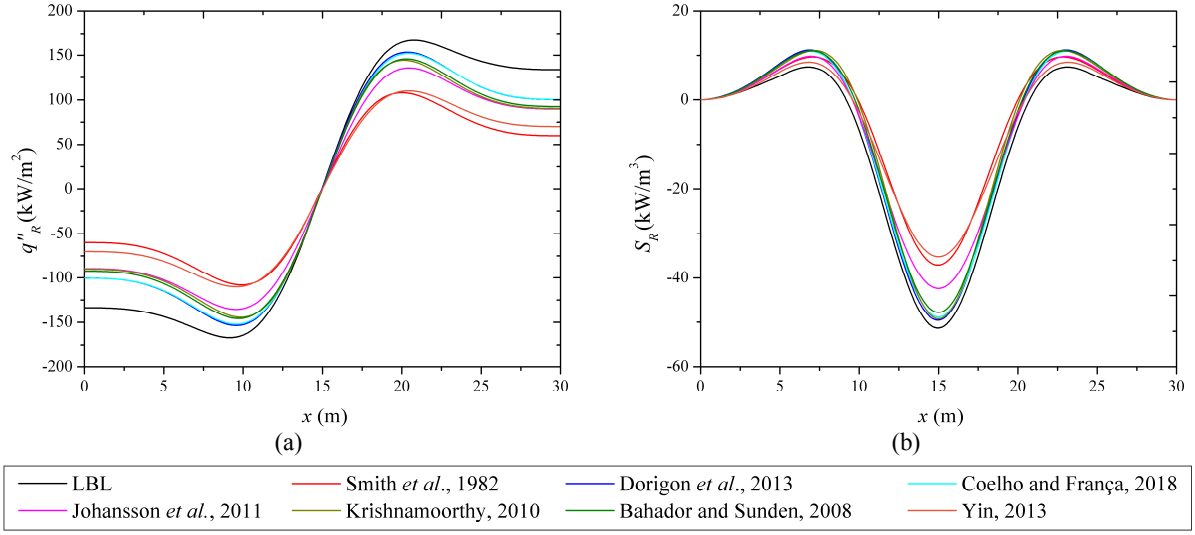

Figure 3. LBL and WSGG solutions for Case 2 with L = 30 m: (a) radiative heat flux; (b) radiative volumetric source.

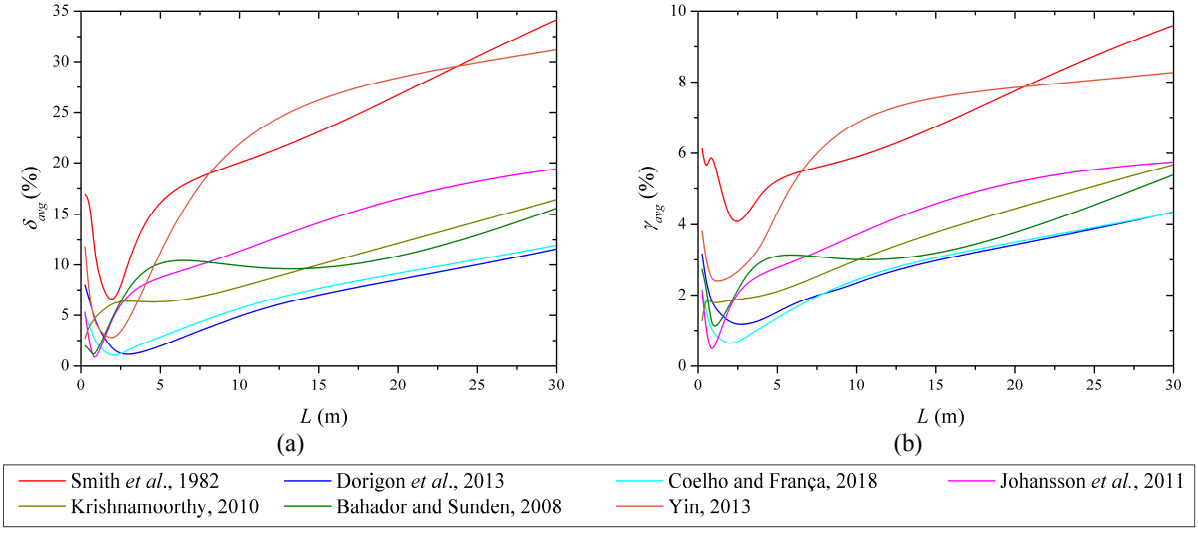

Figure 4. WSGG average deviations as function of L for Case 2 and for: (a) radiative heat flux; (b) radiative volumetric source.

3.3 Case 3

Figure 5 presents the radiative heat flux and volumetric source results for the LBL benchmark and the WSGG solutions with L = 30 m for Case 3. Similar to Case 2, deviations seem to be considerably higher than Case 1, with even the best performing models such as Dorigon *et al.*, 2013 and Coelho and França, 2018 presenting considerably higher

deviations than those reported for lower values of distance between plates L. Smith *et al.*, 1982 and Yin, 2013 models present the highest deviations among others, as also observed in the Cases 1 and 2. However, Fig. 6 shows that the average deviations from both radiative heat flux and volumetric volumetric source in Case 3 are overall lower than those shown in Case 2, for most models analyzed and for most values of L. This indicates that the WSGG predicts these calculations more effectively when the temperature and mole fraction profiles are double symmetrical instead of simple symmetrical, at least for the range of L analyzed in this study. Figure 6a shows that the behavior of the radiative heat flux deviations in Case 3 are similar to the ones observed in Case 2, presenting local minima for low values of L followed by a steady increase as L increases, reaching values higher than 7% for all models and even higher than 15% for Smith *et al.*, 1982 and Yin, 2013 models when L = 30 m. Average deviations from the radiative volumetric source also have local minima for low values of L and increase as L increase, even though the increase is smaller than the one noticed in Case 2, leading to deviations slightly higher than 3% for most models and near 6% for Smith *et al.*, 1982 and Yin, 2013 models when L = 30 m.

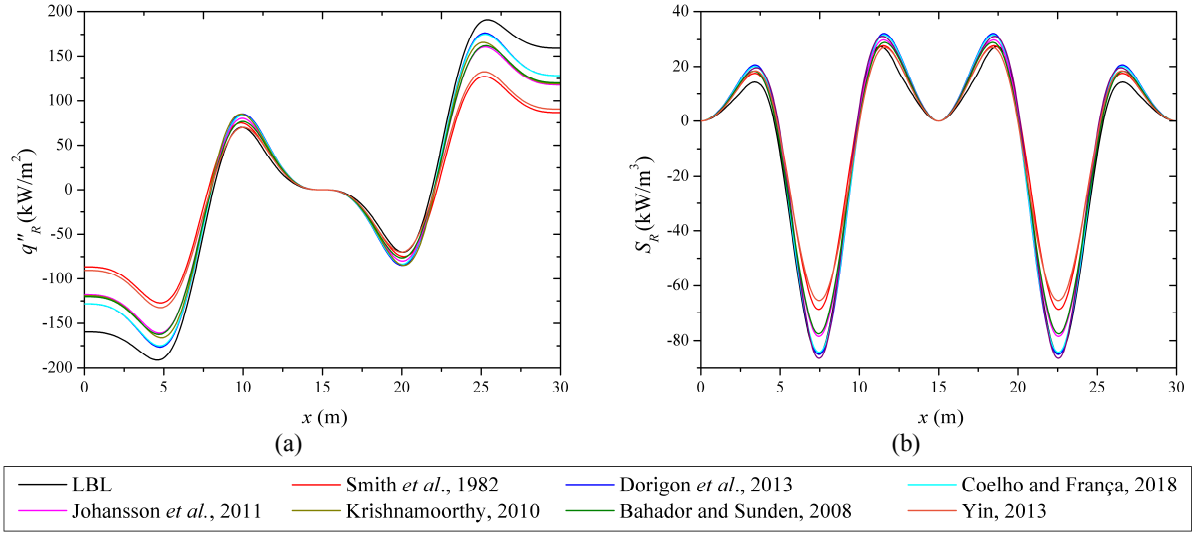

Figure 5. LBL and WSGG solutions for Case 3 with L = 30 m: (a) radiative heat flux; (b) radiative volumetric source.

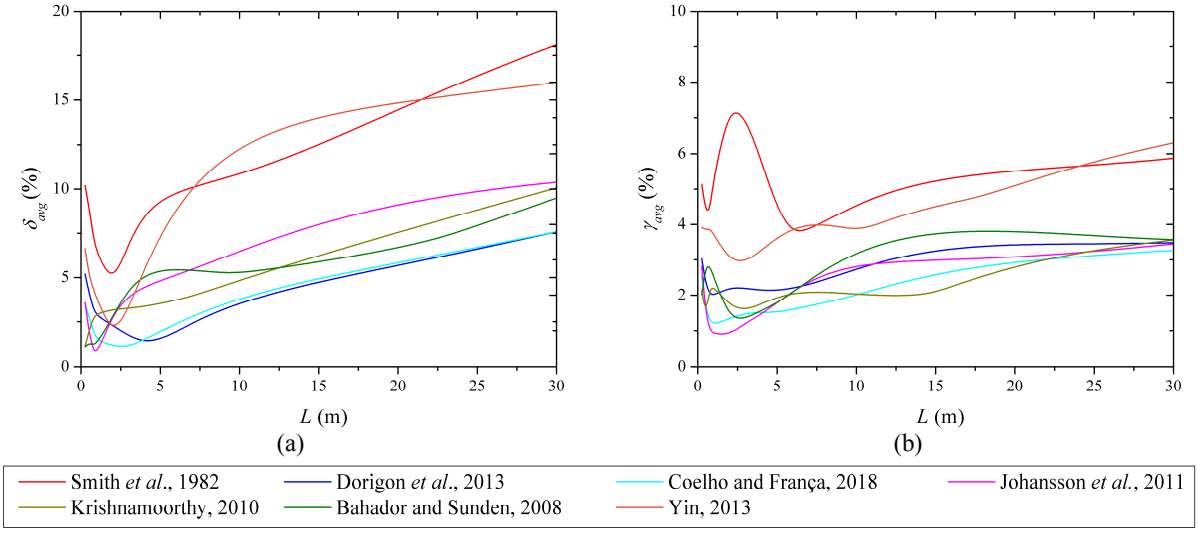

Figure 6. WSGG average deviations as function of L for Case 3 and for: (a) radiative heat flux; (b) radiative volumetric source.

3.4 Case 4

The radiative heat flux and volumetric source results for the LBL benchmark and the WSGG solutions with L = 30 m for Case 4 are presented in Fig. 7. Results for both quantities show deviations similar to those of Case 2 and Case 3, with best performance from Dorigon *et al.*, 2013 and Coelho and França, 2018 models and worst performance from Smith *et al.*, 1982 and Yin, 2013 models. The behavior of the average deviations as a function of L is also very similar, especially to Case 2, as can be seen in Fig. 8. Figure shows that again there is local minima located in low values of L followed by an increase in deviations as L increases, reaching average deviations for L = 30 m between 10% and 32% for the radiative heat flux and between 2% and 7% for the radiative volumetric source. Since the deviations from Case 4 are very similar to those observed in Case 2, it can be concluded that the results are not significantly affected by the asymmetric nature of the temperature and mole fraction profiles and that the PLRAs should be similar to those of Cases 2 and 3.

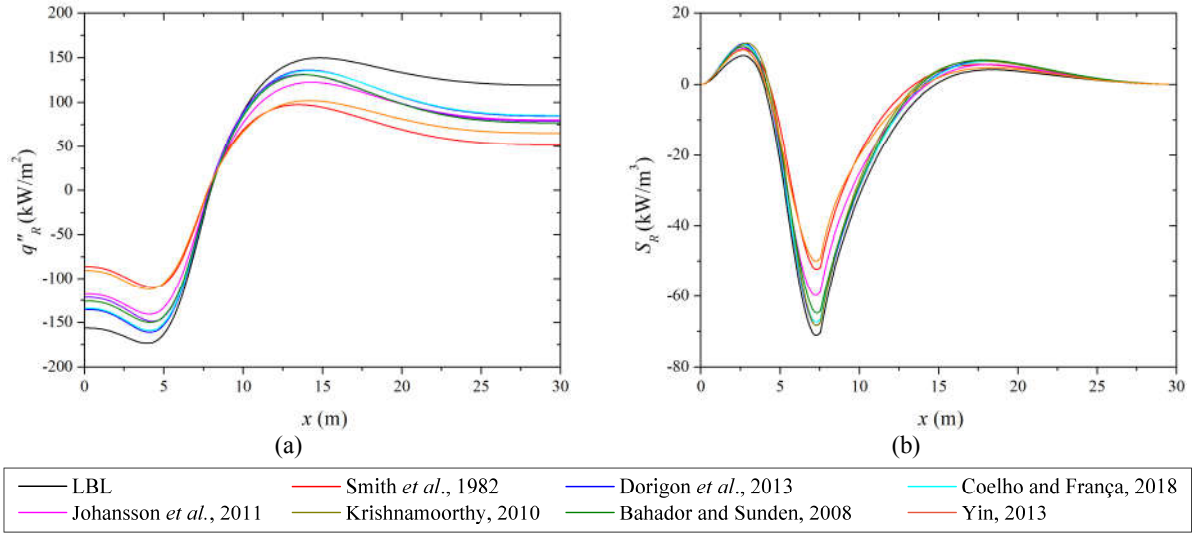

Figure 7. LBL and WSGG solutions for Case 4 with L = 30 m: (a) radiative heat flux; (b) radiative volumetric source.

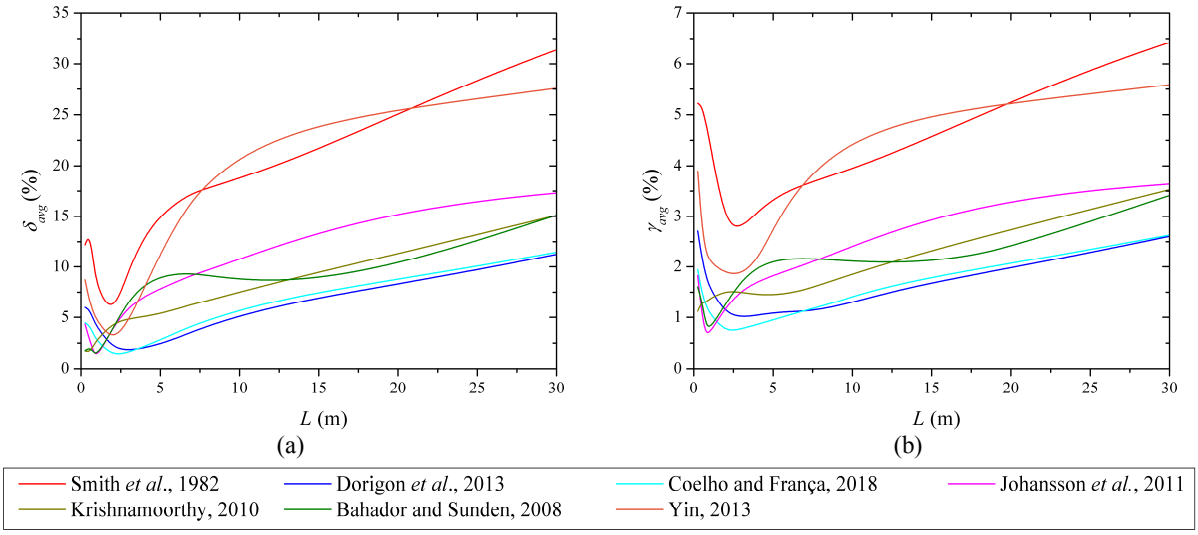

Figure 8. WSGG average deviations as function of L for Case 4 and for: (a) radiative heat flux; (b) radiative volumetric source.

3.5 Path length ranges of applicability (PLRAs)

The PLRAs for average deviations lower than 5% are presented in Table 1. The table shows that PLRAs for radiative heat flux are lower than those for radiative volumetric source for all coefficients studied in this work. This difference between the ranges is due to the higher average deviations involved in radiative heat flux calculations when using the WSGG model, as verified in Figs. 2, 4, 6, and 8. Because of that, for an application where both the radiative heat flux and radiative volumetric source results are important, the PLRA is limited by the radiative heat flux. For Case 1, where temperature and mole fraction profiles are uniform in the domain, only Smith *et al.*, 1982 and Yin, 2013 models are not applicable to the whole range of L for radiative heat flux calculations. However, the PLRAs reduces considerably on the other cases, especially Cases 2 and 4, and even for the best performing models such as Coelho and França, 2018 and Dorigon *et al.*, 2013. For an application where only the radiative volumetric source results are important, the PLRAs increase considerably, as shown in Table 1, with many models being applicable for the whole range of L even on Cases 2-4.

Table 1 - PLRAs for average deviations lower than 5%.

	PLRA (m)			
WSGG Coefficients	Case 1	Case 2	Case 3	Case 4
Radiative heat flux				
Smith *et al.*, 1982	0.25-3, 6-17	-	2	-
Dorigon *et al.*, 2013	0.25-30	1-10	0.5-16	0.75-9
Coelho and França, 2018	0.25-30	0.5-8	0.25-15	0.25-8
Johansson *et al.*, 2011	0.25-30	0.5-1	0.25-5	0.25-2
Krishnamoorth, 2010	0.25-30	0.25-0.75	0.25-10	0.25-3
Bahador and Sunden, 2008	0.25-30	0.25-2	0.25-3	0.25-2
Yin, 2013	0.25-6	1-3	0.75-3	1-3
Radiative volumetric source				
Smith *et al.*, 1982	0.25-30	2-4	0.5-0.75, 5-12	0.75-18
Dorigon *et al.*, 2013	0.25-30	0.25-30	0.25-30	0.25-30
Coelho and França, 2018	0.25-30	0.25-30	0.25-30	0.25-30
Johansson *et al.*, 2011	0.25-30	0.25-18	0.25-30	0.25-30
Krishnamoorthy, 2010	0.25-30	0.25-24	0.25-30	0.25-30
Bahador and Sunden, 2008	0.25-30	0.25-27	0.25-30	0.25-30
Yin, 2013	0.25-30	0.25-5	0.25-19	0.25-15

Table 2 presents the PLRAs for average deviations lower than 10%. Similar to Table 1, the PLRAs are limited by the radiative heat flux, since deviations are overall higher than the ones observed for radiative volumetric source. Table 2 shows that setting the average deviations limit to 10% increases the PLRAs considerably for all cases, with all models being applicable for the whole range of L in Case 1. However, even for deviations of 10%, the models from Smith *et al.*, 1982 and Yin, 2013 still have short PLRAs for Cases 2-4. In fact, most models are not applicable for the whole range of L in Cases 2-4. Tables 1 and 2 illustrate how harder it is to obtain satisfactory accuracy of the WSGG model in radiative heat flux and radiative volumetric source results when compared to total emittance results, especially on problems involving non-uniform mole fraction and temperature profiles. This difficulty is not exclusive to the WSGG model and could probably be observed in other spectral models if similar studies were performed. Results like these also emphasize the importance of studying the dependence of radiative heat flux and volumetric source on path length before recommending PLRAs for WSGG coefficients based on solely total emittance results.

Table 2 - PLRAs for average deviations lower than 10%.

	PLRA (m)			
WSGG Coefficients	Case 1	Case 2	Case 3	Case 4
Radiative heat flux				
Smith *et al.*, 1982	0.25-30	1-2	0.5-6	1-3
Dorigon *et al.*, 2013	0.25-30	0.25-24	0.25-30	0.25-25
Coelho and França, 2018	0.25-30	0.25-23	0.25-30	0.25-24
Johansson *et al.*, 2011	0.25-30	0.25-7	0.25-26	0.25-8
Krishnamoorth, 2010	0.25-30	0.25-15	0.25-29	0.25-16
Bahador and Sunden, 2008	0.25-30	0.25-4, 10-16	0.25-30	0.25-18
Yin, 2013	0.25-30	0.5-4	0.25-6	0.25-4
Radiative volumetric source				
Smith *et al.*, 1982	0.25-30	0.25-30	0.25-30	0.25 to 30
Dorigon *et al.*, 2013	0.25-30	0.25-30	0.25-30	0.25 to 30
Coelho and França, 2018	0.25-30	0.25-30	0.25-30	0.25 to 30
Johansson *et al.*, 2011	0.25-30	0.25-30	0.25-30	0.25 to 30
Krishnamoorthy, 2010	0.25-30	0.25-30	0.25-30	0.25 to 30
Bahador and Sunden, 2008	0.25-30	0.25-30	0.25-30	0.25 to 30
Yin, 2013	0.25-30	0.25-30	0.25-30	0.25 to 30

4. CONCLUSIONS

This study evaluated the accuracy of the WSGG model as a function of path length for non-isothermal, non-homogeneous mixtures of H_2O and CO_2. WSGG coefficients from several authors were analyzed for mixtures with fixed mole ratio of 2/1 and path lengths ranging from 0.25 to 30 m. The coefficients were used to solve the RTE for radiative heat flux and volumetric source and compare it to the LBL benchmark solutions for a one dimensional problem of participating media between two parallel plates. The deviations between the WSGG model and the LBL benchmark were then analyzed as a function of the plate distance varying between the path length range for four different test cases, one with uniform mole fraction and temperature profile and others with non-uniform profiles. Based on these deviations obtained for each test case and each WSGG coefficient, PLRAs were proposed aiming to obtain a maximum of 5% average deviation on the first approach and a maximum of 10% average deviation on the second approach.

Results of radiative heat flux and volumetric source for a plate distance of 30 m are presented for all test cases, showing that Case 1 has considerably lower deviations than the other cases due to the uniform mole fraction and temperature profiles. All the test cases showed that the WSGG coefficients from Smith *et al.*, 1982 and Yin, 2013 presented lowest accuracy while the coefficients from Coelho and França, 2018 and Dorigon *et al.*, 2013 were the best performing overall. Furthermore, deviations between the WSGG coefficients and the LBL benchmark solution were higher in radiative heat flux calculations for all test cases. Results of average deviations for plate distances ranging from 0.25 to 30 m are also presented, showing how the accuracy of radiative heat flux and volumetric source vary as a function of path length for all the coefficients studied. It is verified that the deviations from the radiative heat flux are higher than those of the volumetric source for the whole plate distance range, indicating that the radiative heat flux results should lead to lower PLRAs. Most coefficients presented a local minimum of average deviation in a certain plate distance value, which is different for each set of coefficients. This means that the best performing model depends on the plate distance analyzed, and ideally one would choose the model which has a local minimum near the desired path length. However, after the plate distance range where the local minima are located, deviations from all models seem to follow a smooth pattern and increase with the plate distance. In this region, the best and worst performing models are the similar to the ones previously verified for the plate distance of 30 m.

Finally, PLRAs were determined for maximum of 5% and 10% average deviations for both radiative heat flux and volumetric source. As expected, the PLRAs for radiative heat flux were smaller in both approaches, due to the higher average deviations in the whole path length range. As a consequence, the PLRAs for radiative heat flux were the limiting factor for the WSGG application in all test cases and for all coefficients analyzed in this study. When considering the PLRAs for maximum deviations of 5%, most WSGG models were applicable for the whole path length range in Case 1, while for the other cases even the best performing models were not applicable for the whole range. The

PLRAs for maximum deviations of 10% did increase considerably, but still most models were not applicable for the whole range of plate distance. These results showed that the PLRAs obtained in this work were considerably lower than those recommended by the WSGG coefficients authors, which were based on total emittance calculations. This conclusion emphasizes the importance of studying the dependence of radiative heat flux and volumetric source deviations on path length before recommending PLRAs for WSGG coefficients based solely on total emittance results.

5. ACKNOWLEDGEMENTS

This work has been partially supported by the Brazilian agency CAPES. Research developed with support from the Centro Nacional de Supercomputação (CESUP), Universidade Federal do Rio Grande (UFRGS). Author FRC thanks CAPES (Brazil) for a doctoral scholarship. Author GCF thanks CNPq (Brazil) for a doctoral scholarship. Author FHRF also thanks CNPq (Brazil) for research grants 304728/2010-1 and 473899/2011-6.

6. REFERENCES

Bahador, M. and Sunden, B., 2008. "Evaluation of weighted sum of grey gases coefficients for combustion gases using predicted emissivities from high resolution spectroscopic databases". In *Proceedings of ASME Turbo Expo 2008: Power for Land, Sea and Air – GT2008*. Berlin, Germany.

Bordbar, M.H., Węcel, G., Hyppänen, T., 2014. "A line by line based weighted sum of gray gases model for inhomogeneous CO_2-H_2O mixture in oxy-fired combustion". *Combustion and Flame*, Vol. 161, p. 2435–2445.

Cassol, F., Brittes, R., França, F.H.R., Ezekoye, O.A., 2014. "Application of the weighted-sum-of-gray-gases model for media composed of arbitrary concentrations of H_2O, CO_2 and soot". *International Journal of Heat and Mass Transfer*, Vol. 79, p. 796-806.

Coelho, F.R. and França, F.H.R., 2018. "WSGG correlations based on HITEMP2010 for gas mixtures of H_2O and CO_2 in high total pressure conditions". *International Journal of Heat and Mass Transfer*, Vol. 127, p. 105-114.

Dorigon, L.J., Duciak, G., Brittes, R. Cassol, F. Galarça, M. and França, F.H.R., 2013. "WSGG correlations based on HITEMP 2010 for computation of thermal radiation in non-isothermal, non-homogeneous H_2O/CO_2 mixtures". *International Journal of Heat and Mass Transfer*, Vol. 64, p. 863–873.

Guo, J., Li, X., Huang, X., Liu, Z., Zheng, C., 2015. "A full spectrum *k*-distribution based weighted-sum-of-gray-gases model for oxy-fuel combustion". *International Journal of Heat and Mass Transfer*, Vol. 90, p. 218-226.

Hottel, H.C. and Sarofim, A.F., 1967. Radiation Transfer. McGraw-Hill, New York.

Johansson, R., Leckner, B., Andersson, K., Johnsson F., 2011. "Account for variations in the H_2O to CO_2 molar ratio when modelling gaseous radiative heat transfer with the weighted-sum-of-grey-gases model". *Combustion and Flame*, Vol. 158, p. 893-901.

Kangwanpongpan, T., França, F.H.R., da Silva, R.C., Schneider, P.S., Krautz, H.J., 2012. "New correlations for the weighted-sum-of-gray-gases model in oxy-fuel conditions based on HITEMP 2010 database". *International Journal of Heat and Mass Transfer*, Vol. 55, p. 7419-7433.

Krishnamoorthy, G., 2010. "A new weighted-sum-of-gray-gases model for CO_2-H_2O gas mixtures". *International Communications in Heat and Mass Transfer*, Vol. 37, p. 1182-1186.

Krishnamoorthy, G., 2012. "A new weighted-sum-of-gray-gases model for oxy-combustion scenarios". *International Journal of Energy Research*, Vol. 37, p. 1752-1763.

Rothman, L.S., Gordon, I.E., Barber, R.J., Dothe, H., Gamache, R.R., Goldman, A., Perevalov, V.I., Tashkun, S.A., Tennyson, J., 2010. "HITEMP, the high-temperature molecular spectroscopic database". *Journal of Quantitative Spectroscopy & Radiative Transfer*, Vol. 111, p. 2139-2150.

Siegel, R. and Howell, J., 2002. Thermal Radiation Heat transfer. Taylor and Francis, New York, 4th edition.

Smith, T.F., Shen, Z.F., Friedman, J.N., 1982. "Evaluation of coefficients for the weighted sum of gray gases model". *Journal of Heat Transfer*, Vol. 104, p. 602-608.

Yin, C., Johansen, L.C.R., Rosendahl, L.A., Kær, S.K., 2010. "New weighted sum of gray gases model applicable to computational fluid dynamics (CFD) modeling of oxy-fuel combustion: derivation, validation, and implementation". *Energy & Fuels*, Vol. 24, p. 6275-6282.

Yin, C., 2013. "Refined weighted sum of gray gases model for air-fuel combustion and its impacts". *Energy & Fuels*, Vol. 27, p. 6287-6294.

7. RESPONSIBILITY NOTICE

The authors are the only responsible for the printed material included in this paper.